JOURNAL OF MATERIALS SCIENCE **40** (2005) 5463–5473

Porous aluminum material by plasma spraying

A. DEVASENAPATHI, H. W. NG*, C. M. S. YU, S. W. LIM
Division of Engineering Mechanics, Nanyang Technological University, School of Mechanical and Production Engineering, 50, Nanyang Avenue, Singapore 639798
E-mail: mhwng@ntu.edu.sg

The feasibility of forming porous metallic materials by the plasma spraying process was studied. The process involved the co-spraying of two materials: aluminum (Al) and calcium oxide (CaO), the former being the metallic phase that eventually was retained as the porous structure, while the latter being the sacrificial phase was removed giving rise to pores in the Al matrix. For this the Al and the CaO powders of four different compositions were blended and plasma sprayed on a mold cavity. The CaO was dissolved from the sprayed structure by treating in either water or glycerol. The surface and cross sectional microstructure of the specimens after treatment in water and glycerol showed a more or less uniform pore distribution. The dissolution of CaO, leading to the porous microstructure was confirmed by the X-ray diffractometry. In the XRD spectra, the specimens in the as-sprayed untreated condition exhibited peaks corresponding to both CaO and Al, while, the peaks corresponding to CaO were absent in specimens after water and glycerol treatments confirming CaO dissolution. The study clearly showed that porous aluminum material could be manufactured by plasma spraying.

1. Introduction

Porous metallic materials stand to be a class of materials with a wide range of industrial applications due to their low density, high surface area ratio, high thermal shock resistance and high specific strength [1–3]. Some of the primary engineering applications of porous metals are as filters for catalyst retention, fuel oil burners, medical drug delivery systems, storage reservoirs for liquids such as self-lubricating bearings, heat exchange elements, metallic substrate for solid oxide fuel cells (SOFC), flame and spark arrestors for safe handling of flammable gases used in welding/cutting torch flame arrestors, sound dampening and attenuation as in pneumatic mufflers and silencers [1–5].

The porous metals are manufactured by a variety of powder metallurgy techniques, such as axial compaction and sintering, gravity sintering, isostatic compaction and sintering, metal injection molding and sintering, wet spraying and tape casting [1–7]. Although, some of these manufacturing processes have been well established, certain limitations such as the multiple steps involved and the higher costs demanded alternate methods of manufacturing.

This prompted for the present attempt on a new methodology for forming porous metallic material using plasma spraying as a tool. This approach of porous metal formation by plasma spraying has several advantages, as the process itself is very rapid, with the melting, solidification and compaction of the metal taking place in one step. In addition, the process is versatile in that the porous metals of complex geometry can be obtained, by depositing on an appropriate mandrel shape for the deposition to take place. A study by Kelly *et al*. [8] showed that the porous foam structure can be obtained by spraying a metal in conjunction with a powder which decomposes on contact with the molten metal using the Osprey process. In the present attempt, a different approach of spraying two different blended powders and subsequently dissolving out the soluble phase from the structure to create porous morphology has been utilized. Aluminum (Al) powder was blended with the calcium oxide (CaO) powder under different compositions and plasma sprayed. After spraying, the CaO was dissolved from the specimen by a solvent. Therefore, the formation of porous metallic material involved two steps, firstly, obtaining the specimen by the plasma spraying of the blended powders and the secondly, the subsequent dissolution of CaO in water or glycerol to obtain a porous structure. The CaO was chosen as the soluble second phase material, primarily due to its availability and lower cost, higher melting point (2927°C) [9], which resists decomposition in the high plasma temperature and the lower cost involved with the solvents and equipment to dissolve it.

2. Experimental procedure

The Al powder supplied by Metallisation Ltd., UK and the CaO powder supplied by Goodrich Chemical Enterprise USA were used for the present study. The particle size analysis of the powders was carried out in a Fritsch particle size analysette 22. The particle size of Al was

*Author to whom all correspondence should be addressed.
0022–2461
DOI: 10.1007/s10853-005-2009-5

TABLE I Plasma spray condition and the powder composition used for the present study

Plasma gas	Ar/60 psi
Arc current	400–600 A
Arc voltage	35 V
Spray distance	80 and 120 mm
Carrier gas	Ar/20 psi
Powder feed rate	1.5–12 gm/min
Traverse speed	100 mm/s, 5 mm/step
Mold mandrel	Mild steel - S45C
Powder composition	90 wt.% Al + 10 wt.% CaO
	80 wt.% Al + 20 wt.% CaO
	70 wt.% Al + 30 wt.% CaO
	60 wt.% Al + 40 wt.% CaO

in the range of 10–90 μm with a mean size of 40 μm and CaO was in the range of 5–20 μm with a mean size of 12 μm. The powders under four different wt.% compositions were blended in a rotating ball mill for 24 h and used for spraying. The plasma spray conditions and the powder composition in wt.% used for the study are given in Table I. A specially fabricated mold cavity to retain the shape of the sprayed component along with a release set-up was used. Two different mold cavities namely, the conical openings shown in Fig. 1a and the tile shaped openings (Fig. 1b) with the respective dimensions of 10 mm height by 10 mm base diameter by 8 mm top diameter and 20 mm length by 20 mm width by 5 mm height were machined on a mild steel plate. This plate was then mounted on a backing plate (Fig. 1c) to cover one side of the openings to form a cavity. The plates were then attached to a linear traverse rig and spraying was carried out to fill the cavity of the mold plate. A commercially available high temperature mold release agent was initially sprayed over the mold and the back holding plate prior to plasma spraying for the smooth release of the specimens. After spraying, the top plate was removed from the backing plate to release the sprayed shapes. For each spray condition, at least, three specimens were obtained. The tile and conical specimens obtained are shown in Fig. 1d.

The sprayed specimens were treated in a glass beaker containing 1000 ml of water to dissolve the CaO phase. During, this process, bubble formation was observed on the specimen surface, indicating a dissolution reaction. The CaO can undergo dissolution in water with the formation of calcium hydroxide and hydrogen as shown the following equation:

$$CaO + 2H_2O \longrightarrow Ca(OH)_2 + H_2$$

In order to accelerate the CaO dissolution, the water treatment was carried out in an ultrasonic cleaner operated at a temperature of 80°C, until the evolution of gas bubbles was completely stopped. The advantage of using ultrasonic cleaner is that the loosely held particles in the specimen can be easily dislodged into the solution under the ultrasonic vibration thus enhancing the

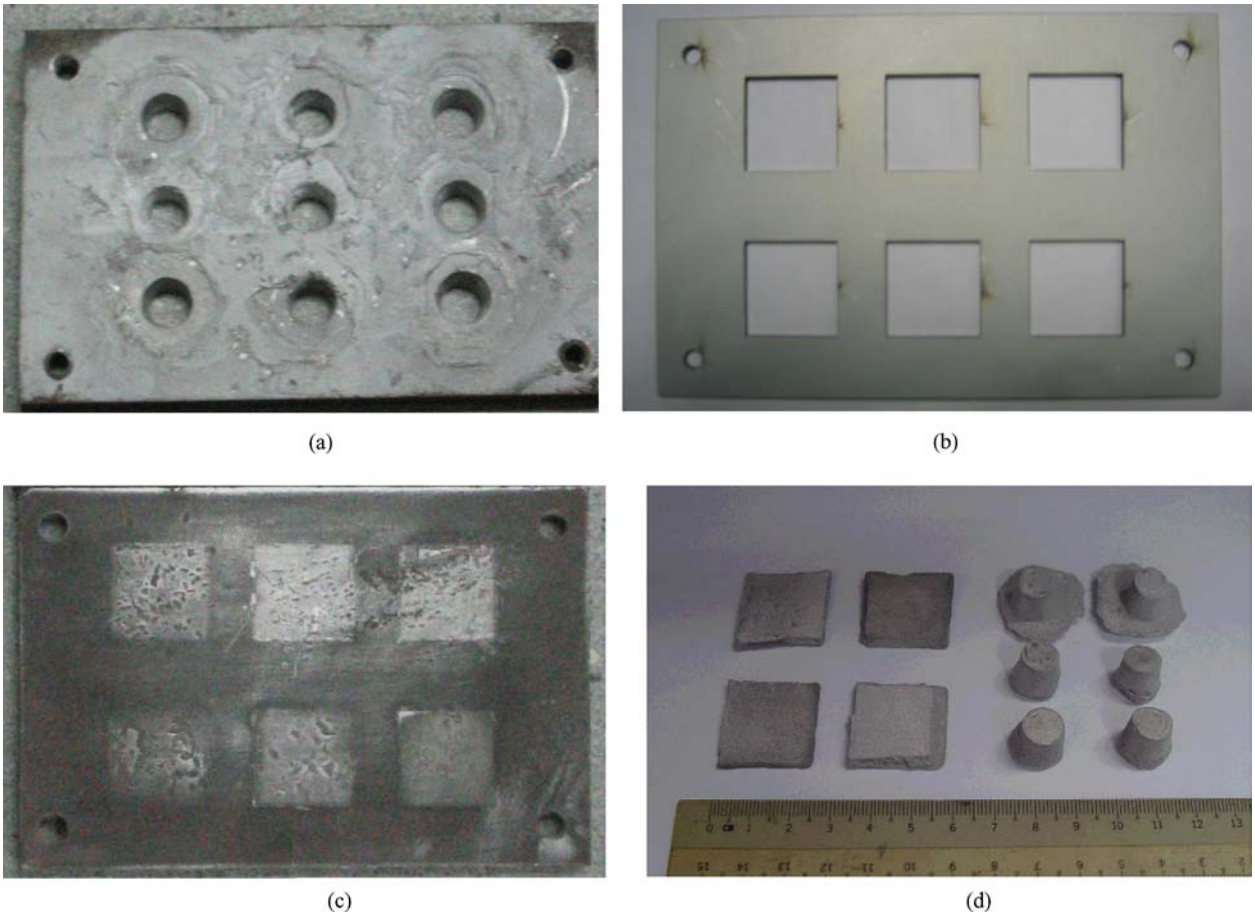

Figure 1 (a) Plate with conical openings for spraying conical specimens (b) Plate with square opening for tile specimens, (c) The backing plate to support the deposits and form cavity during spraying and (d) Plasma sprayed flat and conical shaped specimens produced.

dissolution process. As the CaO is known to undergo complete dissolution in glycerol, the specimens were ultrasonically treated in glycerol solution at a temperature of 80°C, until the bubble formation had completely ceased. The specimens were then cleaned in acetone and cut at the center using a diamond cut-off wheel. The sections were hot mounted using acrylic resin for surface and cross sectional microstructure examination. The mounted specimens were grounded to 1000 grit finish using sand paper and subsequently polished with 6 and 3 μm size diamond paste to a mirror finish. The surface microstructure and elemental mapping were carried out using a JEOL—Model 5600 LV scanning electron microscope (SEM), equipped with the elemental analysis by X-ray diffraction (EDAX). The specimens were subjected to X-ray diffractometry analysis using a Philips X-ray diffractometer. For XRD analysis, the flat specimens were utilized due to their ease of mounting on the machine. The specimens in the as-sprayed condition and after treatment in water and glycerol were analyzed for the presence of Al, CaO and other possible new phases in the XRD operated at a voltage of 30 KV and a current of 20 A.

In order to find out the efficiency of the process, a deposition efficiency study for each powder blend was carried out and compared with that of the Al powder. For this, the spraying was carried out on a flat mild steel specimen for one minute (1 min), which was weighed prior to and after the spraying. The difference in the weight of the specimen before and after spraying was taken as the weight of the alumimium porous foam deposited. In a similar way, the weight of the powder injected through the powder feeder tube for 1 min was measured by collecting the powder in a pre-weighed closed container to get the measure of the flow rate of powder exiting the torch. The ratio between the weight of the powder deposited and the weight of powder exiting the torch during the spraying process gave a measure of deposition efficiency [10].

3. Results and discussion

The flat and conical shaped specimens obtained were subjected to SEM and XRD examinations, the results of which are discussed in the following sections.

3.1. SEM

The microstructure of feedstock powders used for spraying is shown in Fig. 2a–d. Fig. 2a shows the angular shape of Al and Fig. 2b, the CaO powder with some agglomeration. The blending of the Al and CaO leads to CaO being adhered to the Al particles as shown in

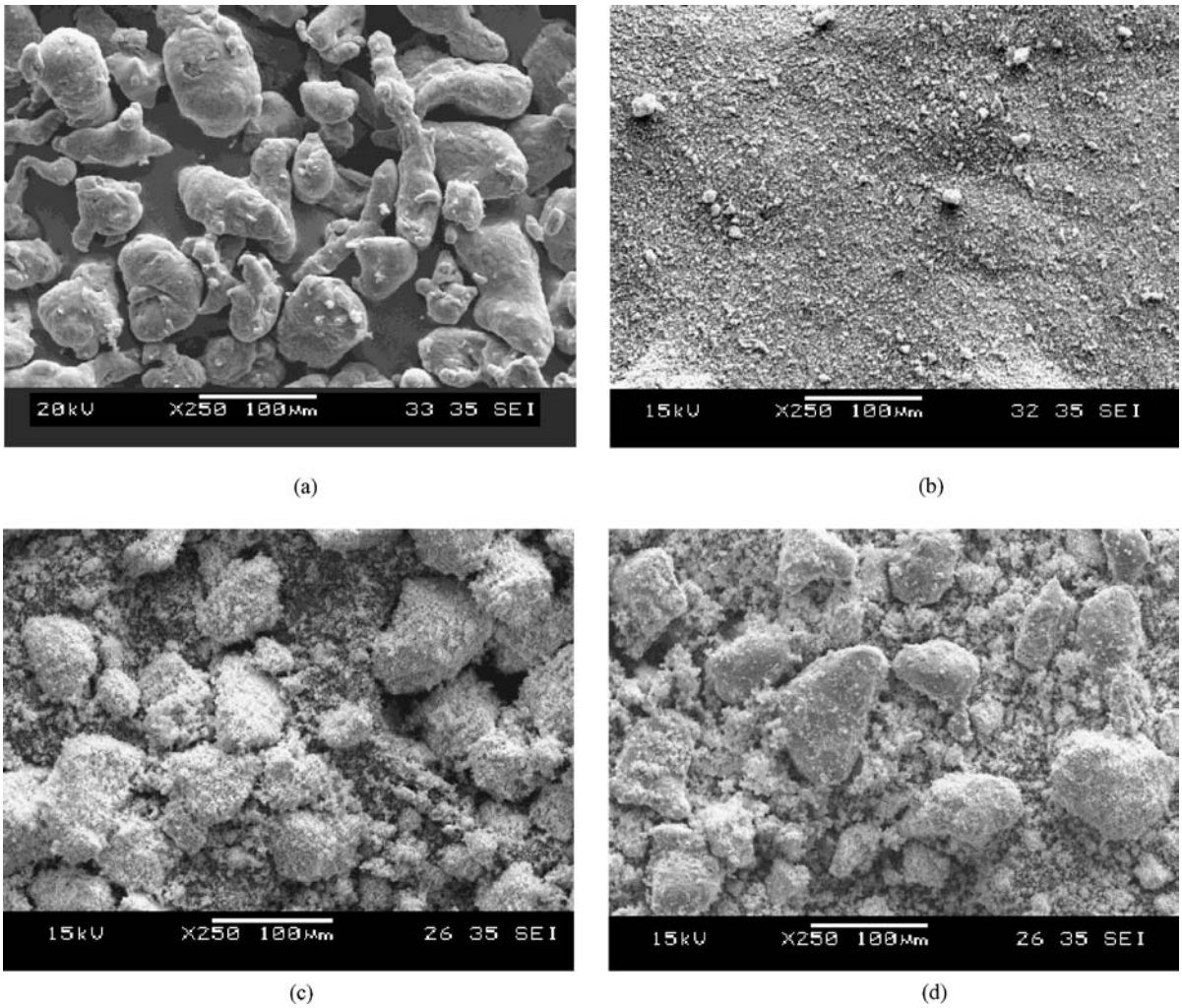

Figure 2 SEM microstructure of powders shows (a) the angular shaped Al (b) the CaO with some agglomeration, complete blending of Al and CaO of (c) 70 wt.% Al + 30 wt.% CaO and (d) 60 wt.% Al + 40 wt.% CaO composition.

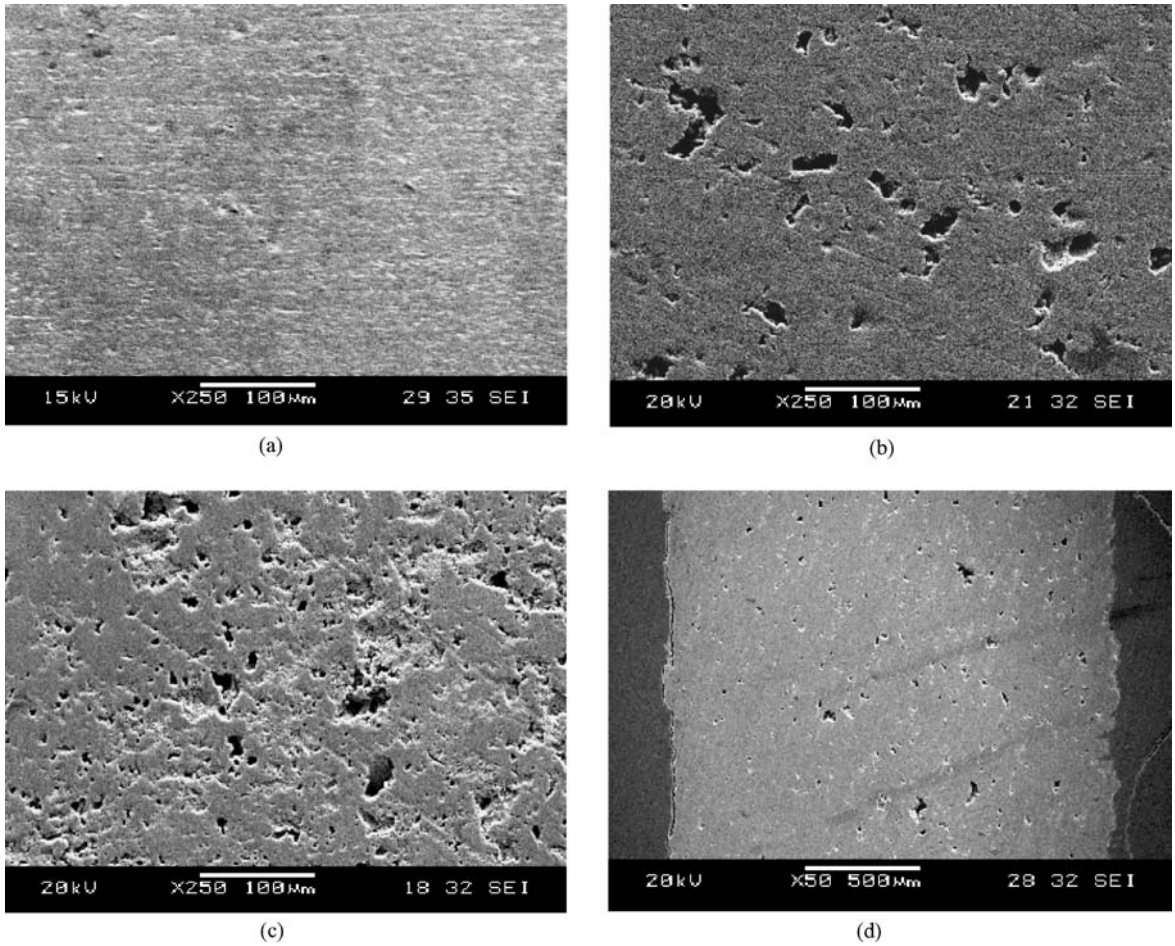

Figure 3 The surface microstructure of the flat specimen obtained with 90 wt.% Al + 10 wt.% CaO in the (a) as-sprayed untreated condition showing no pores, (b) after water treatment, (c) after glycerol treatment and (d) the cross sectional microstructure after water treatment showing pores throughout the specimen.

Figs 2c and d, for the blended powders of compositions of 70 wt.% Al + 30 wt.% CaO and 60 wt.% Al + 40 wt.% CaO. A similar structure was observed for blended powders of other two compositions.

The surface and the cross sectional microstructure of the flat specimen obtained with 90 wt.% Al + 10 wt.% CaO, in the as-sprayed untreated condition and after treatment in water and glycerol is shown in Fig. 3a–d. The as-sprayed specimen (Fig. 3a), shows a smooth texture with the presence of some second phase particles on the surface. The microstructure of specimens after treatment in water (Fig. 3b) and glycerol (Fig. 3c) shows a porous structure throughout the surface. The cross sectional microstructure of the specimen (Fig. 3d), cut at 10 mm from the edge after treating in water, shows the presence of pores throughout, indicating the penetration of water even into the inner layers resulting in the dissolution of CaO. The porous morphology observed throughout the cross-section and the surface implies that the CaO is dissolved out during the water and glycerol treatments.

The surface microstructure of the conical shaped specimen obtained with 80 wt.% Al + 20 wt.% CaO powder, in the as-sprayed condition and after treatment in water and glycerol is shown in Fig. 4a–c. The as-sprayed specimen shows (Fig. 4a), the presence of protruding CaO particles on the smooth specimen surface. This CaO, during treatment in water and glycerol undergoes dissolution giving rise to more or less uniform pore morphology throughout as seen from Figs 4b and c.

This surface and cross sectional microstructure of specimens shown in Figs 3a–d. and 4a–c, indicates that the water or glycerol have penetrated well below the surface of the specimens by a process of infiltration via the microfissures or interconnected pores. It is noted that some of the pores appeared to be closed entirely, yet do not have any CaO present after treatment. The question arises as to the route by which the water or glycerol reaches the pore. The pores observed from the perspective of one half of a cross section (Fig. 3d), indicate that the other half of the section also contain the fissures or interconnected pores to allow the dissolution to take effect. It is also possible that these pores occurred not by CaO dissolution but rather by the gas entrapment during the plasma spraying itself, which is a common phenomenon, in plasma spraying. Another possibility is a corrosion reaction between Al and water, i.e., the pores are corrosion pits left after the dissolution process.

In order to verify whether the observed porosity had resulted from a possible corrosion reaction of Al during water treatment rather than the dissolution of CaO, or the above mentioned causes, the following test was carried out. The Al feed stock powder, without CaO addition was plasma sprayed and the sprayed specimen was allowed to undergo corrosion in water for 40 h after

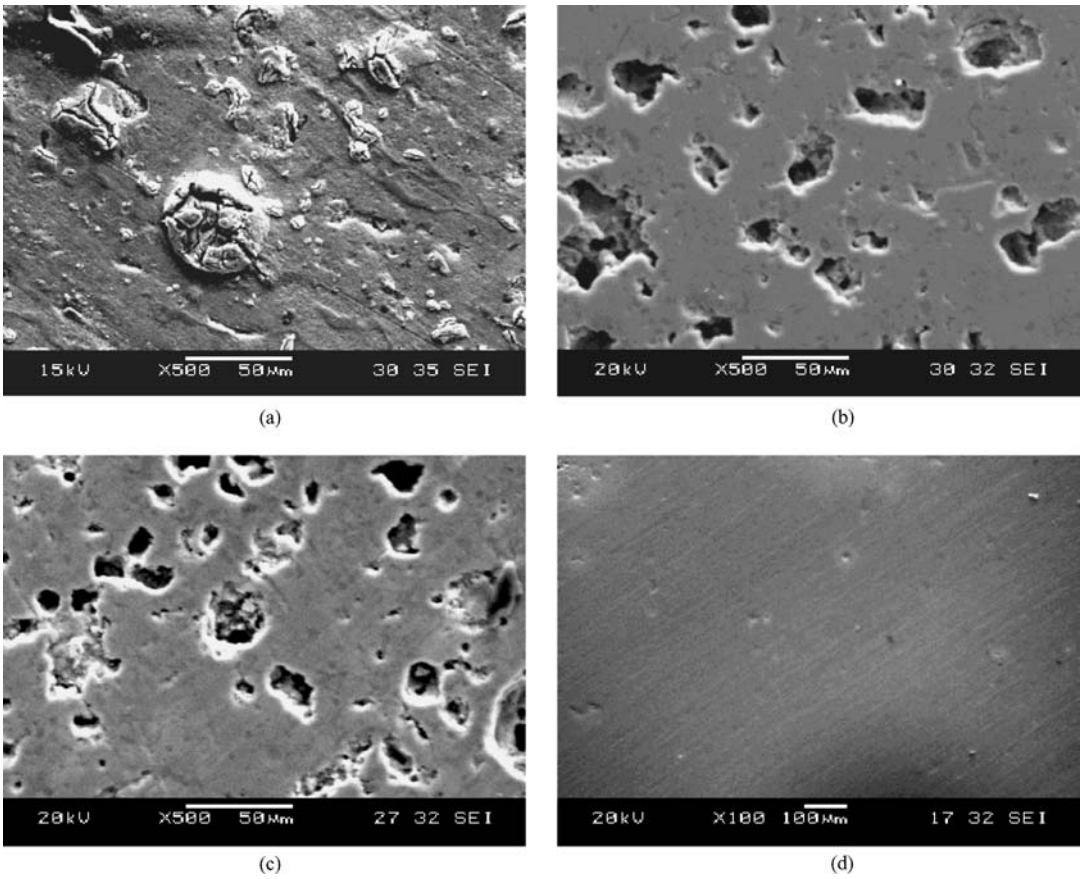

Figure 4 The surface microstructure of the conical shaped specimen obtained with 80 wt.% Al + 20 wt.% CaO in the (a) as-sprayed condition shows no porosity, (b) after treatment in water and (c) glycerol showing the presence of pores. (d) shows the result of corrosion test carried out with Al specimen for 40 h in water showing no pores.

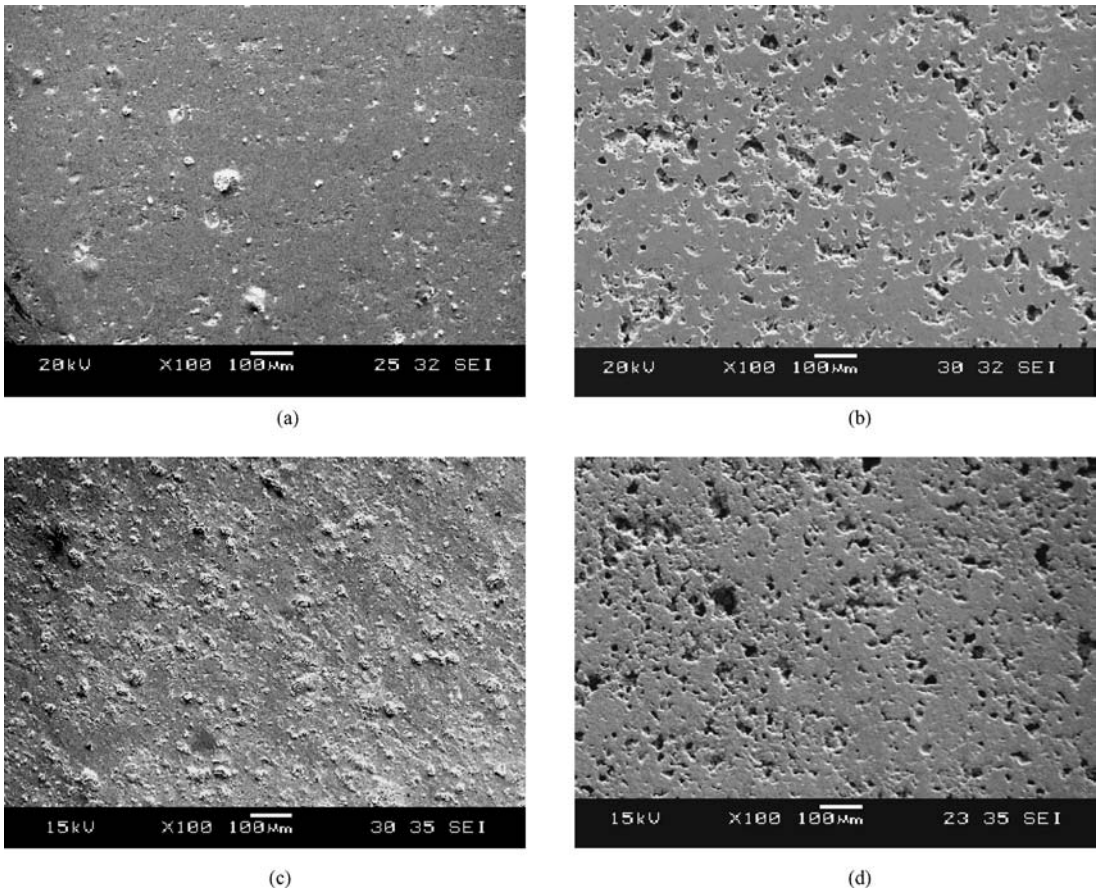

Figure 5 A comparison of the microstructure of conical shaped specimens with CaO particles in the untreated condition and uniform pores after glycerol treatment with the (a) and (b) representing 70 wt.% Al + 30 wt.% CaO and (c) and (d) 60 wt.% Al + 40 wt.% CaO respectively.

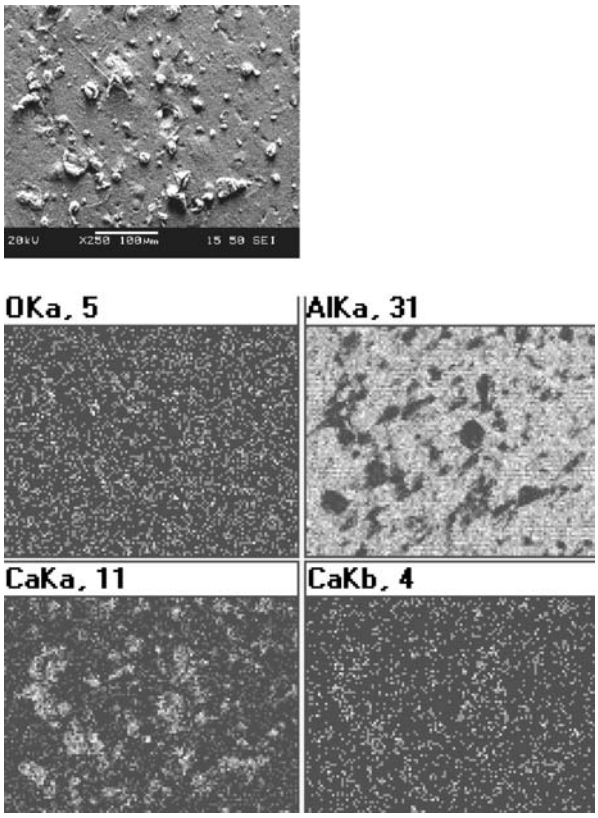

Figure 6 SEM micrograph of the as sprayed 70 wt.% Al + 30 wt.% CaO specimen with the EDAX mapping for the elements oxygen, Al and Ca.

polishing. The specimen microstructure when observed under a microscope (shown in Fig. 4d), did not show pores as observed for the specimen obtained from the blended powders of Al and CaO. This evidence negated the role of corrosion, indicating the dissolution of CaO as a sole reason for the pore formation. This also confirmed that the porosity were not due to gas entrapment in the plasma spraying process.

The effect of percentage CaO in the composition of the blends on the extent of pore formation is further examined from the microstructure of conical shaped specimens sprayed with 70 wt.% Al + 30 wt.% CaO and 60 wt.% Al + 40 wt.% CaO powders as shown in Fig. 5a–d. The microstructure of the untreated specimens (Fig. 5a and c) and the specimens treated in glycerol (Fig. 5c and d) are shown in the figure. A clear difference in the extent of porosity is observed between the specimens sprayed with 70 wt.% Al + 30 wt.% CaO and 60 wt.% Al + 40 wt.% CaO, with the latter exhibiting a higher number of pores. In comparison with the microstructure of specimens obtained from powders of 80 wt.% Al + 20 wt.% CaO and 90 wt.% Al + 10 wt.% CaO, the extent of porosity increases with increase in CaO content.

The retention of CaO in the as-sprayed specimen and its role in forming the pores after dissolution was further confirmed by the EDAX studies. The SEM microstructure of the as-sprayed conical shaped specimen obtained from the 70 wt.% Al + 30 wt.% CaO powder

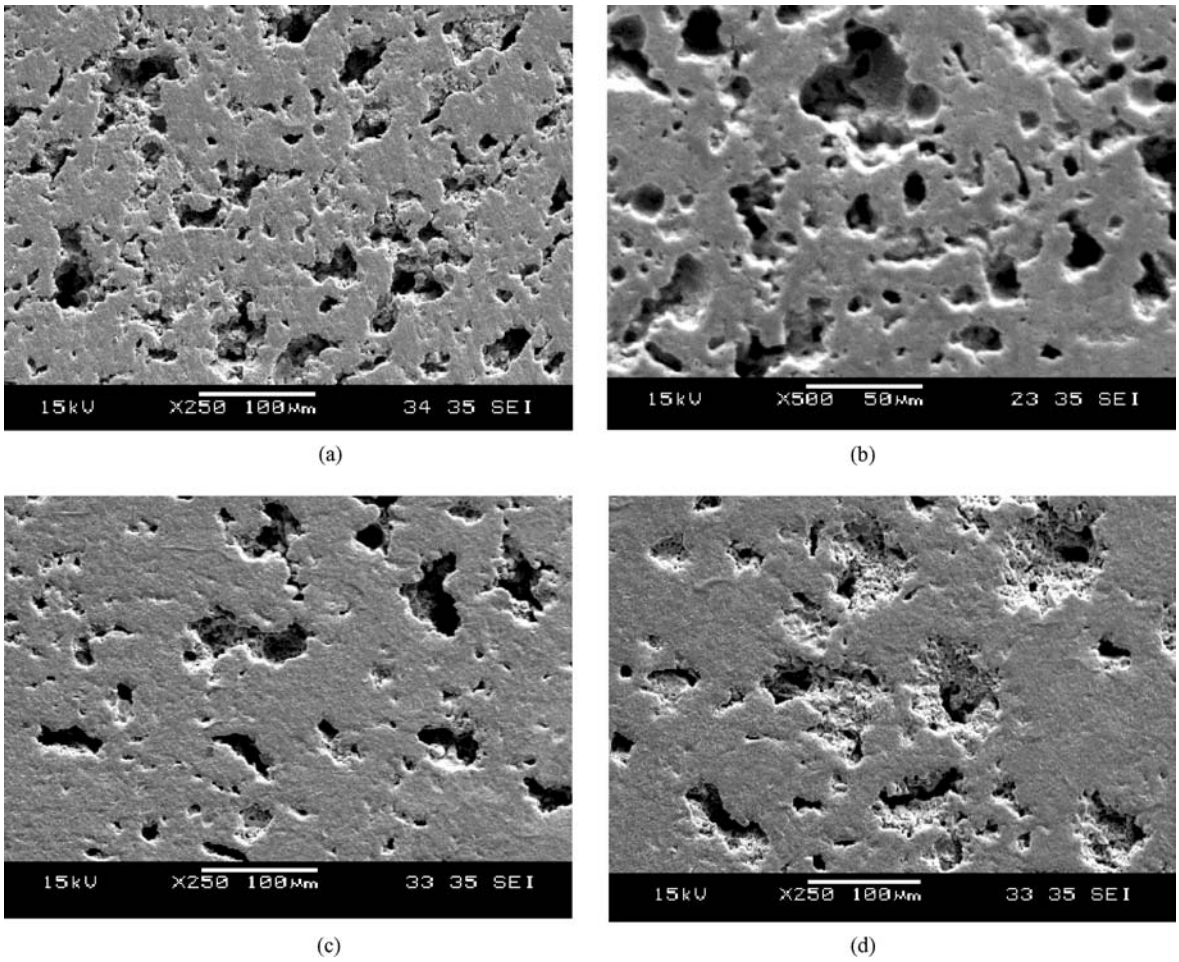

Figure 7 The effect of arc current on the extent of porosity of specimens sprayed with 60 wt.% Al + 40 wt.% CaO powder after treatment in water. (a) and (b) showing the specimen sprayed at 400 A with a large number of pores with interpenetrating network, (c) and (d) showing a decrease in the extent of porosity for specimens sprayed at 500 and 600 A respectively.

and its elemental mapping results by EDAX are shown in Fig. 6. The SEM microstructure clearly shows the white patches of particles spread over the surface of the specimen. The EDAX mapping for oxygen shows its presence throughout, indicating the spread of CaO over the surface, as the oxygen peaks corresponds to the oxygen from CaO. Although for the case of Al, it is is well spread throughout the surface, there are specific areas where it is completely absent. In the case of Ca, the mapping shows the presence of Ca throughout the surface, with the tendency to concentrated at locations where the Al was absent. The mapping results show that although the powders are well blended before spraying, accumulation of CaO at certain areas occurs during the spraying. The dissolution of this accumulated CaO during water or glycerol treatments could give rise to larger sized pores with the smaller sized pores arising from the dissolution of the uniformly distributed CaO from other areas.

The effect of arc current on the extent of porosity was studied from the cylindrical specimens of 60 wt.% Al + 40 wt.% CaO powder sprayed at 400, 500 and 600 A current. Fig. 7a–d shows the microstructure of the specimens after water treatment in which it is seen that the surface microstructure of specimen (Fig. 7a and b) which is sprayed at 400 A arc current, shows higher number of pores with an interpenetrating network. However, for higher levels of arc current up to 500 A (Fig. 7c) and 600 A (Fig. 7d), a decrease in the extent of porosity with shallow pores is observed. A possible reason for this, is the increase in the extent of melting of Al powder with higher arc current [10, 11]. As the completly melted Al powder, could form more dense, compact and interconnected splats at higher arc currents of 500 and 600 A, it is expected that the penetration of water or glycerol into the inner layers is restricted to some extent. As the CaO present in the outer layers are easily dissolved out, the CaO present

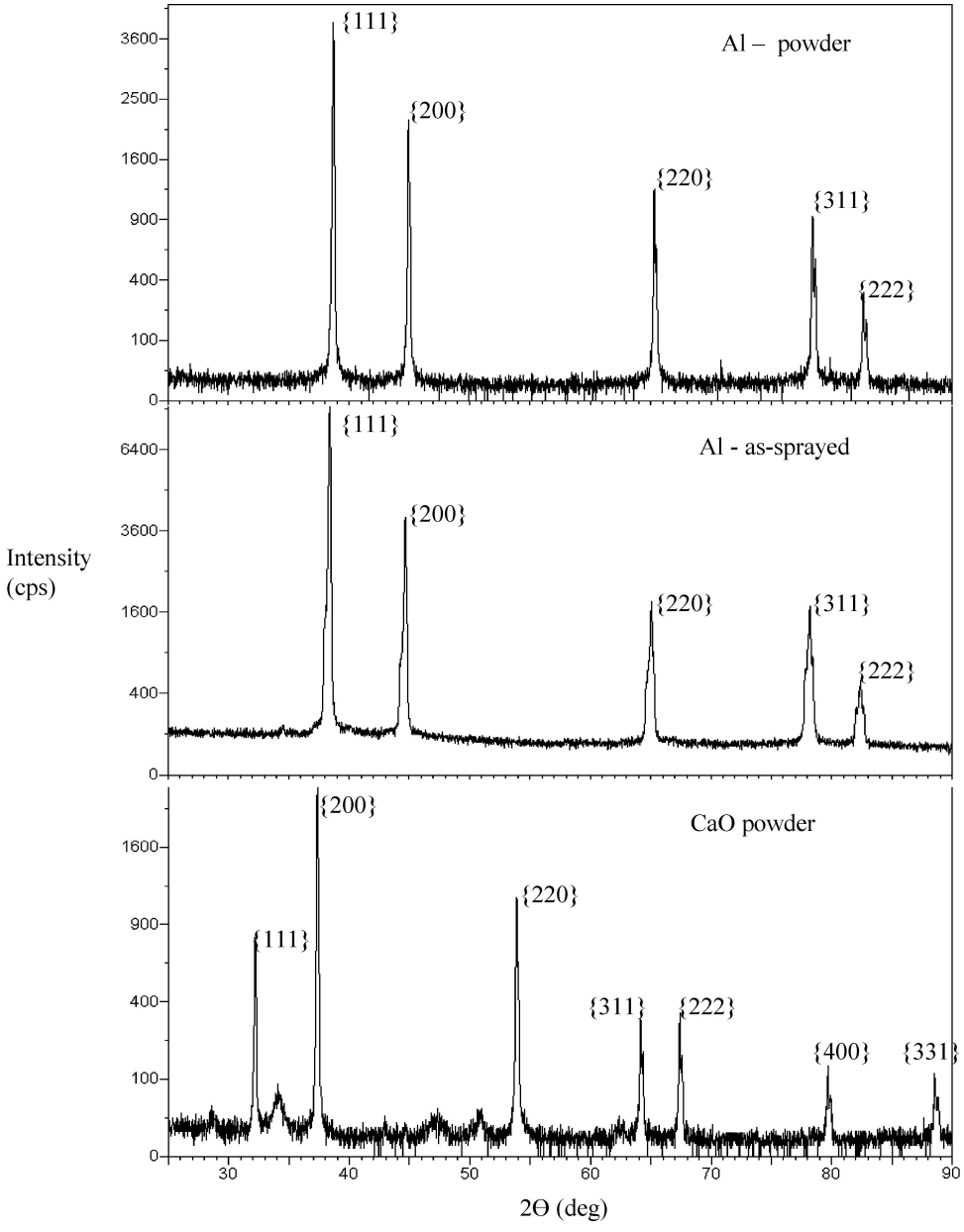

Figure 8 Showing the XRD patterns of Al feedstock, Al in the as-sprayed condition and CaO feedstock. Presence of peaks corresponding to Al feedstock powder in the case of as-sprayed Al shows the absence of any oxidation during the plasma spraying.

in the inner layers are not completely so. This could lead to retention of CaO in the specimen, giving rise to a lower porosity (Fig. 7c and d). A similar, change in microstructure with arc current was observed in the case of glycerol treated specimens also, indicating the role of arc current in controlling the extent of porosity.

3.2. XRD spectra

XRD spectroscopy is used to reveal the elemental composition of the Al powder, Al in the as-sprayed condition and the CaO powder. From the XRD spectra shown in Fig. 8, it is observed that in the spectra for Al feedstock powder and as-sprayed Al specimen, only the peaks corresponding to the Al is presented. This clearly indicates a very little or no oxidation during the spraying process, which otherwise is normally a problem encountered in the sintering process [12]. As the plasma spraying is a rapid process, where the melting, solidification and compaction of the molten droplets takes place within a fraction of second, the oxidation of Al is minimized signifying the superiority of this process.

The XRD spectra of the specimens obtained from the 90 wt.% Al + 10 wt.% CaO powder in the as-sprayed condition and after the water and glycerol treatments is shown in Fig. 9. The untreated as-sprayed specimen shows the peaks corresponding only to Al and CaO, ruling out the formation of any other new phase or intermetallic compounds during the plasma spraying of the blended powders. This also confirms the retention

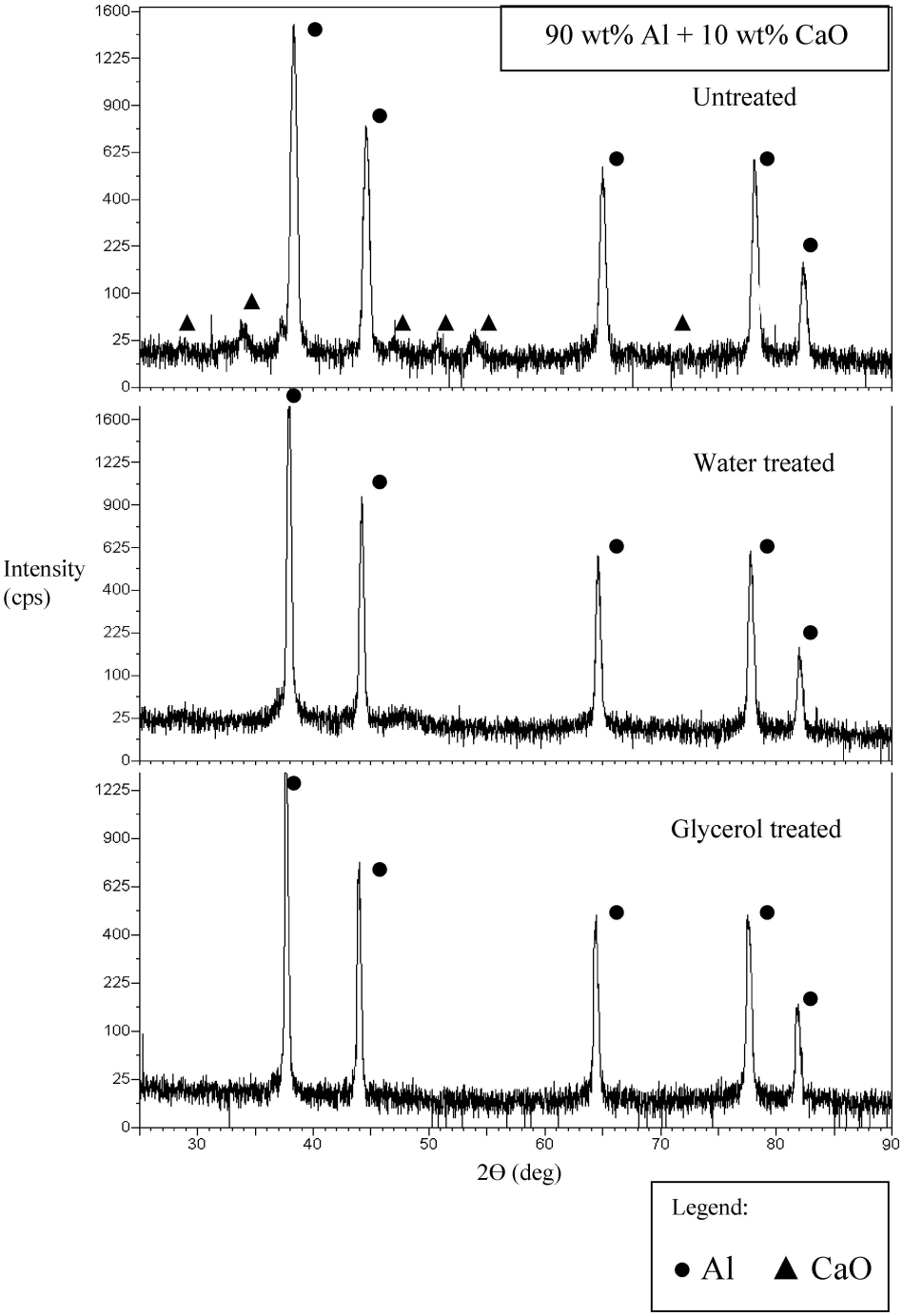

Figure 9 XRD patterns of specimen sprayed with 90 wt.% Al + 10 wt.% CaO powder, shows the presence of CaO peaks in the untreated as-sprayed specimen and its absence after the water and glycerol treatments indicating the dissolution of CaO.

of Al and CaO in their original form. In water and glycerol treated specimens, the peaks corresponding to CaO are absent indicating its dissolution.

The XRD spectra of specimens sprayed with powders containing 80, 70 and 60 wt.% of Al and the corresponding 20, 30 and 40 wt.% CaO, also shows the presence of CaO in the untreated specimens and its absence in the water and glycerol treated ones. A representative XRD spectra obtained with 70 wt.% Al + 30 wt.% CaO is shown in Fig. 10. The figure indicates the presence of CaO in the as-sprayed specimens without any treatment, following treatment with water and glycerol leads to the dissolution of CaO as observed from the absence of peaks corresponding to CaO.

Fig. 11, shows the effect of arc current on the nature of the porous structure. The specimens formed at 400 A current shows the absence of CaO after water treatment, while the specimens obtained at 500 A and 600 A shows peaks corresponding to CaO even after the water treatment. Furthermore, the intensity of peaks corresponding to increase of CaO for the specimen obtained at 600 A compared to that obtained at 500 A, shows the slight retention of CaO even after the water treatment. A possible reason for this observed increase in CaO content with the increase in arc current is that of the increased plasma plume temperature, which in turn increase the extent of melting of Al particle resulting to a closer compaction and buildup of the splats. This

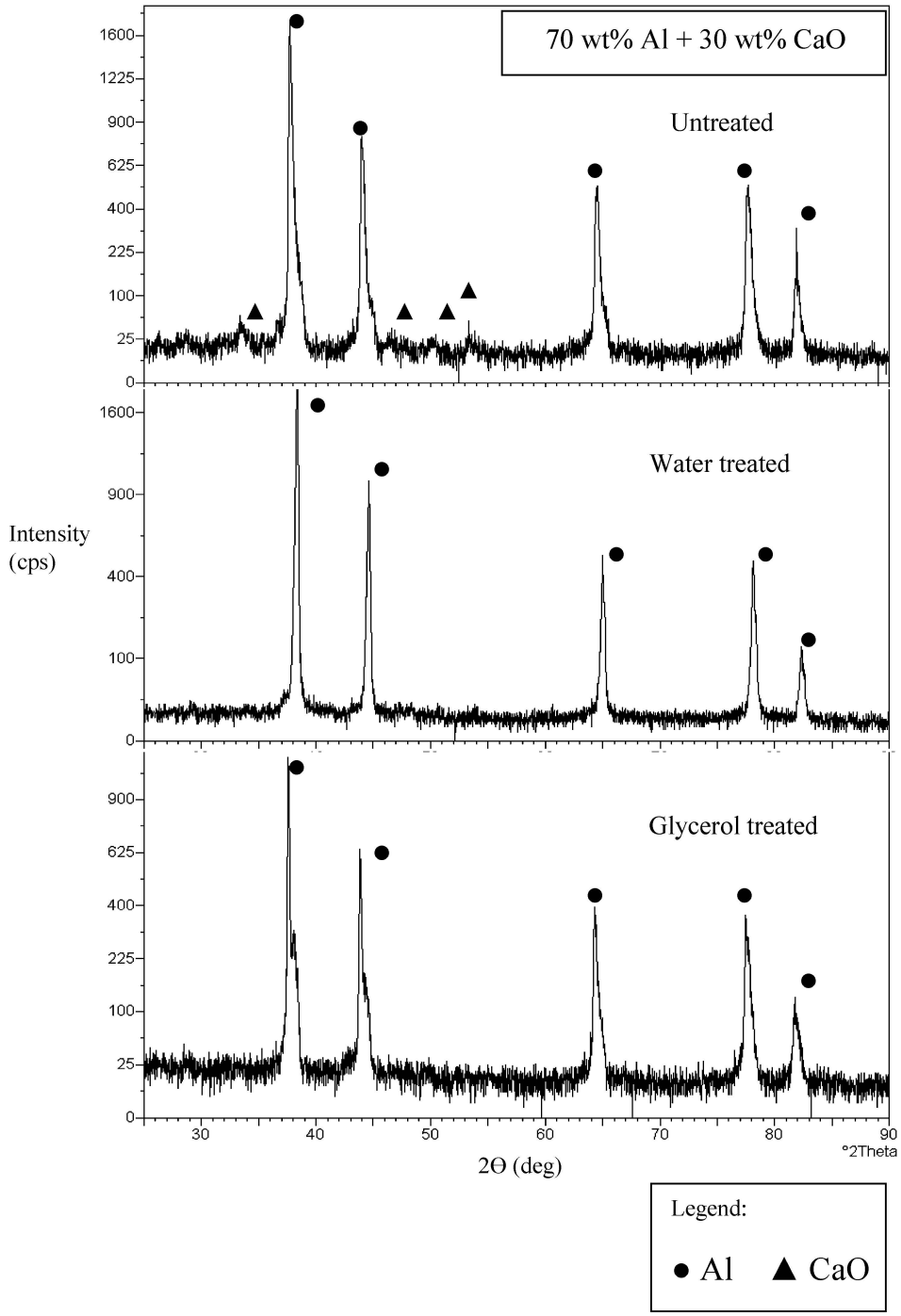

Figure 10 Shows the presence of CaO in the untreated as-sprayed specimen and its absence in both the water-treated and glycerol-treated specimens sprayed with 70 wt.% Al + 30 wt.% CaO powder.

could reduce the ability of water or glycerol penetrating to the inner layers and reaching the CaO to dissolve it, resulting only in partial dissolution.

3.3. Effect of powder composition on deposition efficiency

The effect of powder composition and the arc current on the deposition efficiency of is shown in Fig. 12. The Al shows the highest deposition efficiency of slightly over 70%, which decreases with the addition of CaO. A steady decrease in the deposition efficiency is observed with the increase in CaO content. One reason for the observed phenomena is the high melting point (2927°C) of CaO, which could undergo only partial melting or remain unmelted during the spraying. This in turn leads to a poor adherence between Al splats and CaO splats, affecting the specimen build-up. Thus, the decrease in deposition efficiency observed with the increase in CaO content is due to the decrease in the adherence of the powder particles. The effect of arc current on the deposition efficiency is shown in Fig. 12. In general, for all the powder compositions a decrease in the deposition efficiency is observed with the increase in arc current. The reason for this is that with increase in the arc current the plasma plume temperature increases leading to complete melting and vaporization of the sprayed Al particles due to its low melting point (660°C). Since

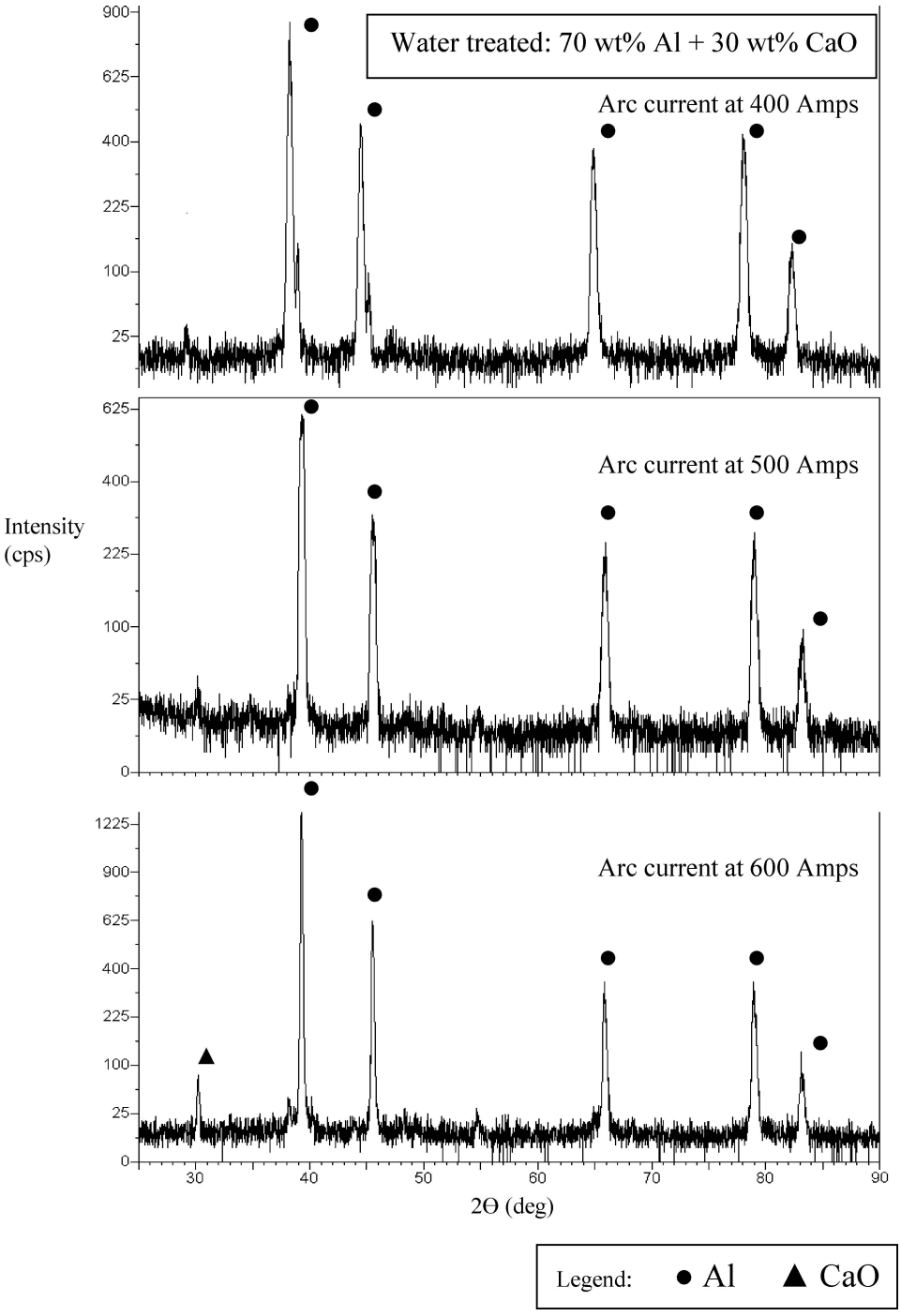

Figure 11 Shows the XRD results of water treated specimens sprayed at the arc current of 400 A and 500 A current showing the absence of CaO peaks, which sprayed at at 600 A shows the presence of peaks corresponding to CaO sprayed with 70 wt.% Al + 30 wt.% CaO powder.

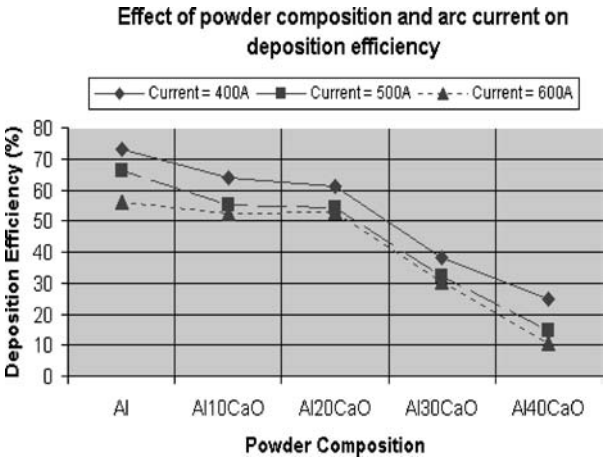

Figure 12 Shows the effect of powder composition and arc current on the deposition efficiency.

the deposition efficiency is dependent on the particle's state [10], the particles vaporized with increase in arc current lowers the deposition efficiency.

The present feasibility study, demonstrates that plasma spraying can be successfully utilized for forming porous Al material. The roles of powder composition and arc current on the extent of porosity in the Al-CaO system were investigated. From the SEM micrographs, a clear relation between the CaO content and the extent of porosity has been observed. The role of CaO in determining the extent of porosity was clearly observed in the increased porosity in the specimens with the increase in the CaO content. The effect of arc current on porosity, was observed from the decrease in the extent of porosity in the specimens sprayed at higher arc currents of 500 and 600 A.

One of the limitations with the present process is the long time (40 h) taken for the dissolution of CaO. This can be easily overcome either with the use of proper solvents and temperature to accelerate the process of CaO dissolution or using an easily dissolvable powder in the place of CaO. The use of a polymer that would withstand the plasma temperature during spraying and its subsequent dissolution in a solvent is yet another alternative. A more detailed study in relating the extent of porosity and density of this material with the powder composition is being carried out as a continuation of this work, the results of which will be reported at a later stage.

4. Conclusions

The present study, demonstrates the feasibility of forming porous Al material by means of plasma spraying of the blended powders of Al and CaO, followed by the dissolution of CaO by treating in water or glycerol. The microstructure and XRD studies confirm the porosity as resulting from the dissolution of CaO from the sprayed material. The CaO content in the sprayed powder is found to determine the extent of porosity as observed from the increased porosity with increase in the CaO content.

References

1. P. S. LIU and K. M. LIANG, *J. Mater. Sci.* **36** (2001) 5059.
2. G. J. DAVIES and SHU ZHEN, *ibid.* **18** (1983) 1899.
3. L. J. GIBSON and M. F. ASHBY, "Cellular Solids," 2nd Ed. (Cambridge University Press, Cambridge, 1997).
4. K. SIZIKI and T. NAKAGAWA, *Engng. Mater.* **30** (1982) 104.
5. M. NANKO, N. FUSAMUNE, K. SHIZAKI, Y. KONDO and H. ONISHI, *J. Por. Materi.* **2** (1995) 157.
6. JIANG, J. CIZERON, J. F. BERTONE and V. L. COLVIN, *J. Am. Chem. Soc.* **121** (1999) 7957.
7. M. NANKO and K. ISHIZAKI, *J. Por. Mater.* **1** (1995) 19.
8. P. KELLEY, C. R. WONG and A. MORAN, *Int. J. Powder Metall.* **29** (1993) 161.
9. N. A. LANGE, in "Lange's Hand Book of Chemistry" edited by John A. Dean (13th Edition, Mc-Graw Hill Book Company, 1985) pp. 4–35.
10. A. DEVASENAPATHI, C. B. ANG, S. C. M. YU and H. W. NG, *Surf. Coat. Technol.* **139** (2001) 44.
11. R. MCPHERSON, *Surf. Coat. Technol.* **39/40** (1989) 173.
12. Y. Y. ZHAO and D. X. SUN, *Scripta Mater.* **44** (2001) 105.

Received 20 May 2004
and accepted 16 February 2005